

Original Research Article

Synthesis and characterisation of doxorubicin-loaded functionalised cobalt ferrite nanoparticles and their in vitro anti-tumour activity under an AC-magnetic field

Muhammad Waheed Mushtaq^{1,2*}, Farah Kanwal², Atif Islam³, Khalil Ahmed², Zia-ul-Haq², Tahir Jamil³, Muhammad Imran², Syed Mustansar Abbas⁴, Qingrong Huang¹

¹Food Science Department, Rutgers, The State University of New Jersey 08901, USA, ²Institute of Chemistry, ³Department of Polymer Engineering and Technology, University of the Punjab, Lahore-54590, Pakistan, ⁴Department of Energy and Materials Engineering, Dongguk University, 30, Pildong-ro, 1-gil, Jung-gu, Seoul 100-715, Republic of Korea

*For correspondence: **Email:** waheedjaami@gmail.com; **Tel:** +92-03045578484

Sent for review: 22 November 2016

Revised accepted: 5 June 2017

Abstract

Purpose: To synthesise and evaluate the anti-tumour properties of doxorubicin-loaded xanthan gum-functionalised cobalt ferrite nanoparticles (CoFe₂O₄.NPs@XG-Doxo) under an AC-magnetic field.

Methods: Multidimensional magnetic cobalt ferrite (CoFe₂O₄) nanoparticles (NPs) were synthesised by a co-precipitation method. The synthesised cobalt ferrite nanoparticles (CFNPs) were functionalised with xanthine gum (XG) and subsequently characterised by Fourier transform-infrared spectroscopy (FT-IR), thermogravimetric analysis (TGA) and contact angle studies. Vibrating sample magnetometry (VSM) was used for magnetic measurements of the native and XG-coated CFNPs. The microstructural morphology of the uncoated and XG-coated CFNPs was established using scanning electron microscopy (SEM), atomic force microscopy (AFM) and dynamic light scattering (DLS) studies. Finally, the doxorubicin release profile of the drug-loaded functionalised CFNPs was evaluated using an oscillating magnetic field (OMF) apparatus in the presence of an externally applied magnetic field.

Results: XG coating decreased the contact angle of the native CFNPs from 92° to 40°, which indicates that it modified the CFNP surface from hydrophobic to hydrophilic. VSM analysis demonstrated that CoFe₂O₄.NPs@XG also retained the magnetic characteristics of the bare cobalt ferrite nanocrystals, endorsing its application as a promising magnetic nanovector (MNV). The synthesised CoFe₂O₄.NPs@XG-Doxo exhibited significantly higher controlled discharge of doxorubicin at acidic pH (5.0) than at neutral pH (7.4). In vitro analysis revealed the remarkable lower systematic toxicity of XG-coated CoFe₂O₄.NPs compared with uncoated CFNPs against Chinese hamster ovary (CHO) and Huh7 cell lines.

Conclusion: These results indicate that XG-coated CFNPs are a biocompatible MNV for doxorubicin.

Keywords: Cobalt ferrite, Cytotoxicity, Drug delivery, Nanoparticles, Xanthan gum

Tropical Journal of Pharmaceutical Research is indexed by Science Citation Index (SciSearch), Scopus, International Pharmaceutical Abstract, Chemical Abstracts, Embase, Index Copernicus, EBSCO, African Index Medicus, JournalSeek, Journal Citation Reports/Science Edition, Directory of Open Access Journals (DOAJ), African Journal Online, Bioline International, Open-J-Gate and Pharmacy Abstracts

INTRODUCTION

Various nanosystems have been proposed to increase their implementation in several biological fields, such as cancer therapy,

pharmaceuticals and tissue engineering [1]. In particular, spinel ferrites (MFe₂O₄, M = Fe⁺², Zn⁺², Mn⁺², Co⁺² or Ni⁺²) are promising magnetic products for many biomedical applications. Cobalt ferrite nanoparticles (CFNPs) are suitable

for magnetic resonance imaging (MRI) and targeted drug delivery (TDD) because of their tunable coercivity and excellent saturation magnetisation (Ms) [2]. There are various routes to prepare CFNPs, such as *via* combustion [3], microemulsions with oil-in-water micelles [4], reverse micelles [5], co-precipitation and calcination [6], sol-gels [7], microwaves [8] and forced hydrolysis in a polyol medium [9].

However, biomedical applications of native CFNPs are restricted because of their hydrophobic surface. Most of the plasma proteins are hydrophobic, which enables the rapid removal of hydrophobic nanostructures from the blood circulatory system through opsonisation [10]. Previously, nanoferrite functionalization was carried out by coating with proteins, polymers, surfactants, starch or chitosan [11]. We report herein the first investigation of encapsulating CFNPs with xanthan gum (XG), which is an anionic polysaccharide that coats the cationic surface of the NPs. The biocompatibility of XG suggests a broad range of applications in the biomedical arena [12].

Herein, we report the synthesis and characterisation of XG-coated CFNPs (CoFe₂O₄.NPs@XG) to enhance application as a biocompatible magnetic nanovector (MNV) for targeted delivery of the anti-tumour drug doxorubicin (Doxo). The release of drug from CoFe₂O₄.NPs@XG-Doxo was determined in the absence as well as in the presence of an externally applied magnetic field (AMF). The cytocompatibility and toxicity of the naked and XG-coated ferrite NPs toward Chinese hamster ovary (CHO) and Huh7 cell lines are also reported.

EXPERIMENTAL

Materials

Cobalt (II) chloride hexahydrate (CoCl₂·6H₂O; Alfa Aesar, 98 % purity), iron (III) chloride hexahydrate (FeCl₃·6H₂O; Sigma–Aldrich, ACS reagent grade, 97 % purity), potassium hydroxide (KOH; Alfa Aesar, 98 % purity), ethanol (C₂H₅OH; Sigma–Aldrich) and doxorubicin hydrochloride (Sigma–Aldrich) were used as received. Double-distilled deionised water was used as solvent.

Synthesis of the CFNPs

The CFNPs were synthesised using a previously reported method with minor modifications [13]. Briefly, aqueous solutions of ferric chloride (0.4 M, 25 mL) and cobalt chloride (0.2 M, 25 mL)

were mixed and stirred in a three-necked flask at pH 1.34. Precipitation occurred immediately as 3 M KOH solution was slowly added drop-wise under an inert atmosphere of nitrogen gas. Then, the reaction temperature was increased to 85 °C and stirring was maintained for 90 min. The resulting dark black precipitate was decanted using a strong permanent magnet, washed multiple times with distilled water and finally oven-dried at 100 °C for 12 h. The synthesised cobalt ferrite nanocrystals were dialysed for 8 h in 100 mL of 0.02 M HNO₃ solution to form a cationic charge over the surface, dried and stored at 4 °C for further functionalization.

Synthesis of MNV (CoFe₂O₄.NPs@XG)

XG-coated CFNPs (CoFe₂O₄.NPs@XG) were prepared by dispersing the dialysed cobalt ferrite nanocrystals in distilled water, mixing with XG at a 1:2 ratio and stirring for 24 h. The supernatant layer was discarded and the resulting dark brown coated cobalt ferrite nanocrystals were washed with distilled water and finally freeze-dried for further studies.

In vitro drug loading and release studies

The prepared MNV (CoFe₂O₄.NPs@XG) was loaded with Doxo by dissolving 10 mg of dried CoFe₂O₄.NPs@XG in 25 mL of a drug solution (0.2 mg/mL) at room temperature and gently stirring for 2 days in the dark. The drug solution was prepared in phosphate-buffered solution (PBS) at pH 7.4. Thereafter, the drug-loaded magnetic nanoassembly, CoFe₂O₄.NPs@XG-Doxo, was separated using a magnet, washed several times with PBS and finally freeze-dried. The supernatant and washed solutions were collected and analysed to determine the unloaded drug concentration by UV-visible (UV-Vis) spectroscopy at a wavelength of 481 nm. The drug loading efficiency (L) was calculated using Eq 1.

$$L (\%) = \frac{Co - C}{Co} \times 100 \dots\dots\dots (1)$$

where Co is the total amount of the added drug and C is the unencapsulated amount of drug.

To determine the drug release profile, 6 mg of the drug-loaded MNV (CoFe₂O₄.NPs@XG) was sealed in a porous dialysis bag having a molecular weight cut-off (MWCO) of 10 kDa (Millipore). Thereafter, the dialysis bag was suspended in 40 mL of sterile phosphate-buffered solution having pH 7.4 and 5.0 separately at 37 °C under gentle orbital shaking (120 rpm/min). At designated time intervals (1, 2, 4, 6, 8, 10, 12, 24, 36, 48, 20, 24, 36, 48, 60, 72,

84, 96, 108 and 120 h), 2 mL of dialysate was withdrawn from the dialysis bag to determine the released drug concentration. The withdrawn volumes of dialysate were returned to the release medium to reconstitute the original volume of PBS. In a similar fashion, the drug release experiment was repeated when the drug release system was placed in a 40-mL glass tube in the presence of an external oscillating magnetic field (OMF) (ca. 1000 Oe) generated by a custom-made instrument called a Teslamate. This device (Figure 1) consisted of 96 turns of a 76.5-mm length of 0.8-mm-diameter copper wire that operated over a frequency of 1–500 kHz at a current of 1–3 amperes and a magnetic flux density of 0–100 mG.

Cell cultures

The CHO and Huh7 cell lines were provided by the Centre of Excellence and Molecular Biology (CEMB), Lahore, Pakistan. To obtain culture growth, the cell lines were maintained in Dulbecco's modified Eagle's medium (DMEM) supplemented with 10 % foetal bovine serum (FBS) and incubated at 37 °C under a humidified atmosphere containing 5 % CO₂. The cells lines were routinely harvested by adding 0.25 % trypsin–ethylenediaminetetraacetic acid (EDTA) solution.

Cytotoxicity of the MNV (CoFe₂O₄.NP@XG)

To analyse the *in vitro* cytotoxicity of the bare and coated cobalt ferrite NPs against CHO and Huh7, cells were harvested in 96-well plates at a density of 10,000 cells per well. Different concentrations of native CoFe₂O₄.NPs and CoFe₂O₄.NPs@XG (0–2.0 mg/mL) were added to each well, in duplicate. Thereafter, the culture plate was incubated at 37 °C in humidified air

containing 5 % CO₂ for 48 h. After culturing sufficient cells, the medium in all wells was exchanged with fresh medium. Finally, the standard MTT (3-(4,5-dimethylthiazol-2-yl)-2,5-diphenyltetrazolium bromide) assay was used to measure the cell viability relative to that of the control untreated cells.

In vitro cytotoxicity of the magnetic nanoassembly (CoFe₂O₄.NPs@XG-Doxo)

The *in vitro* cytotoxicity of the drug-loaded magnetic nanoassembly, CoFe₂O₄.NPs@XG-Doxo, was tested against the Huh7 cell line by MTT assay. Briefly, 1 × 10⁴ cells/well were harvested in a 96-well plate and incubated at 37 °C with humidified air containing 5 % CO₂ for 24 h. Then, different concentrations (0–0.20 mg/mL) of the drug-loaded magnetic nanoassembly were added to each well medium, in triplicate, and incubated in 5 % CO₂ humidified air at 37 °C for 24 h to determine cell viability.

UV-visible spectroscopy

The UV-vis spectra of the pure cobalt ferrite NPs were recorded in the range of 100–600 nm using a spectrometer (model UV-2600; Shimadzu, Japan). The drug loading and release profile was also obtained with the same instrument at 481 nm.

Fourier transform-infrared (FT-IR) spectroscopy

The FT-IR spectra of the cobalt ferrite NPs and its nanocomposites were recorded on a spectrophotometer (model 983; Perkin-Elmer, USA) using the KBr technique in the range of 400 – 4,000 cm⁻¹.

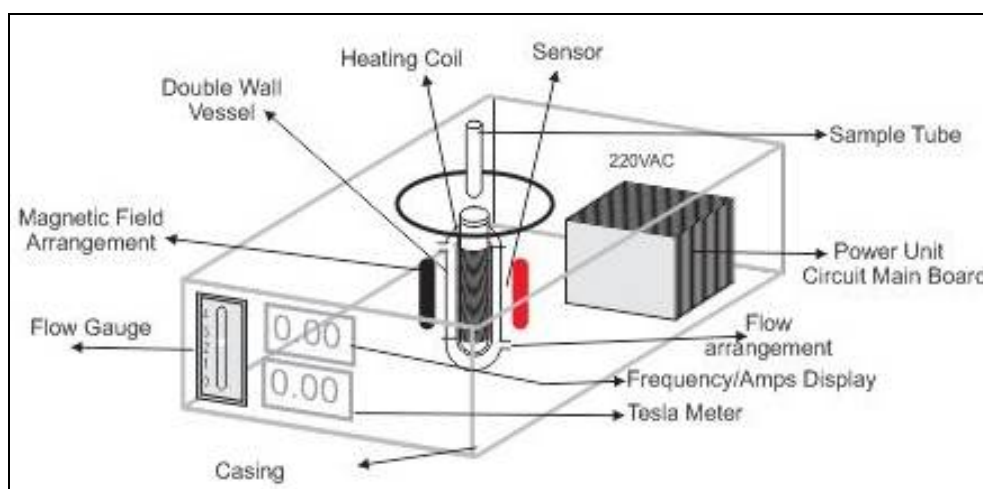


Figure 1: Teslamate used to generate oscillating magnetic field (OMF) for drug release studies

Thermogravimetric analysis (TGA)

The thermal properties of the native cobalt ferrite NPs and the weight percentage of XG coated on the NPs were determined by TGA (model TGA-50; Shimadzu, Japan) over the range of 20 – 800 °C.

Contact angle measurements

The contact angles of uncoated and XG-coated cobalt ferrite NPs were measured using a contact angle meter with the sessile drop method (model HO-ED-M-01, Holmarc Opto-Mechatronics, India).

X-ray diffraction (XRD) studies

XRD patterns were measured with a diffractometer (model 6000; Shimadzu, Japan) in the 2θ range of 5–70° using Ni-filtered Cu-K α radiation. The crystallite size was determined from the broad diffraction plane (311) using the Debye–Scherer equation (Eq 2) [14]:

$$D = \frac{k\lambda}{\beta \cos\theta} \dots\dots\dots (2)$$

where k is a constant (0.9), β is the full-width at half-maximum (FWHM) of the high-intensity diffraction peak corresponding to the (311) plane, λ is the wavelength of the Cu K α radiation (1.54 Å) and θ is the Bragg angle.

Vibrating sample magnetometry (VSM)

The magnetic potential of coated and uncoated CoFe₂O₄.NPs was evaluated using a vibrating sample magnetometer (model 7404; Lake Shore Cryotronics, USA) at 300 K at an AMF ranging from –15 to 15 KOe.

Microstructural analysis

The microstructures of prepared samples were studied by scanning electron microscopy (SEM; model TM-1000; Hitachi, Japan). Atomic force microscopy (AFM; Park NX10, Korea) was used to measure the size of native and coated ferrite particles dispersed in hexane. The hydrodynamic diameter and polydispersity index (PDI) of a sample was measured by dynamic light scattering (DLS; Zetasizer Nano S; Malvern, UK).

RESULTS

UV-vis spectra

The successful synthesis of the cobalt ferrite NPs by co-precipitation was initially confirmed by UV-

Vis spectroscopy. The nanoferrite spectra displayed a characteristic shoulder band in the range of 330–500 nm that was attributed to their synthesis [15] (Figure 2).

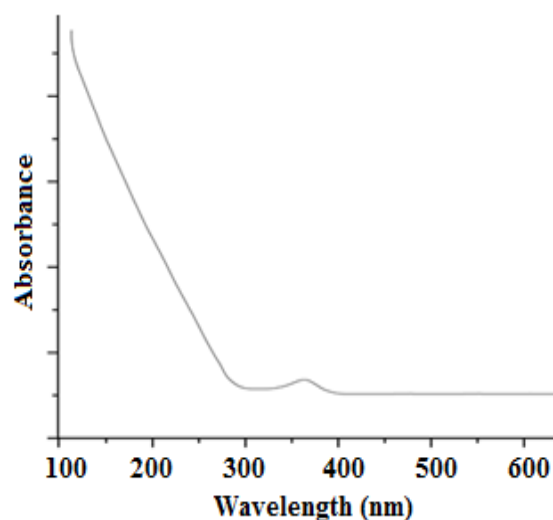


Figure 2: UV-visible spectrum of native cobalt ferrite NPs (CoFe₂O₄.NPs)

Attenuated total reflectance (ATR) FT-IR spectra

The CFNPs and their XG-coated derivative (CoFe₂O₄.NPs@XG) were investigated by ATR FT-IR spectroscopy. Figure 3 shows the spectra of the uncoated and coated CFNPs. The characteristic spinel-phase peaks of native cobalt ferrite NPs observed at 610 and 492 cm⁻¹ were attributed to the intrinsic vibration of (M–O)_{th} and (M–O)_{oh} sites, respectively [16]. The splitting of the low-frequency band at the octahedral (B) site revealed the presence of different metal ions including Fe³⁺, Fe²⁺ and Co²⁺. The broad absorption band at 3350–3500 cm⁻¹ was assigned to the stretching vibration of the –OH group. Figure 3b shows the presence of the ferrite spinel lattice band at 400–600 cm⁻¹, which confirmed the coating of XG over the ferrite NPs. The additional bands at 1447 and 1072 cm⁻¹ correspond to the M–O–C linkage (M = Co, Fe) [17]. Various quinone and ketone carbonyl peaks confirmed the loading of Doxo onto the coated CFNPs (Figure 3c). The splitting of the 2950–3250 and 1547 cm⁻¹ peaks correspond to the N–H stretching and N–H bending vibrations, respectively, of the secondary amide group. In brief, the FT-IR spectrum of the loaded drug (Figure 3c) revealed the drug adsorption in two ways: first, by partial interaction between the XG carboxylate (COO⁻) and amine (–NH₂) groups of the drug *via* amide formation and, second, by the –OH vibrational bands.

Table 1: Significant infrared stretching frequencies

Sample	IR region or band (cm ⁻¹)	Characteristic vibration*
CoFe ₂ O ₄ .NPs	3480	ν_s (O-H)
	610	ν_s (CoFe ₂ O ₄) _A , A-site
	492, 438	ν_s (CoFe ₂ O ₄) _B , B-site
CoFe ₂ O ₄ .NPs@XG	3600–3000	ν_s (O-H)
	2930, 2840	ν_{as} (C-H) and ν_s (C-H), xanthan gum
	1639	δ (H-O-H), free or absorbed water
	1526	ν_{as} (OCO ⁻), free carboxylic group
	1447, 1072	ν_s (M-O-C), M = Fe, Co
	1160	acetal group, xanthan gum
	596	ν_s (CoFe ₂ O ₄) _A , A-site
	474, 432	ν_s (CoFe ₂ O ₄) _B , B-site
CoFe ₂ O ₄ .NPs@XG-Dox	3560–3160	ν_s (O-H), hydrogen-bonded
	3160–2300	ν_{as} (C-H), ν_s (C-H)
	2076	ν_s (C=O), ketone group
	1617	δ (H-O-H), free or absorbed water
	1547	(N-H), secondary amide
	1117	(C-O), tertiary alcohol
	1036	(C-O), secondary alcohol
	872	-NH ₂ , primary amine
	584	ν_s (CoFe ₂ O ₄) _A , A-site
	470	ν_s (CoFe ₂ O ₄) _B , B-site

* ν_s , symmetric stretching; ν_{as} , asymmetric stretching; δ , scissoring vibration

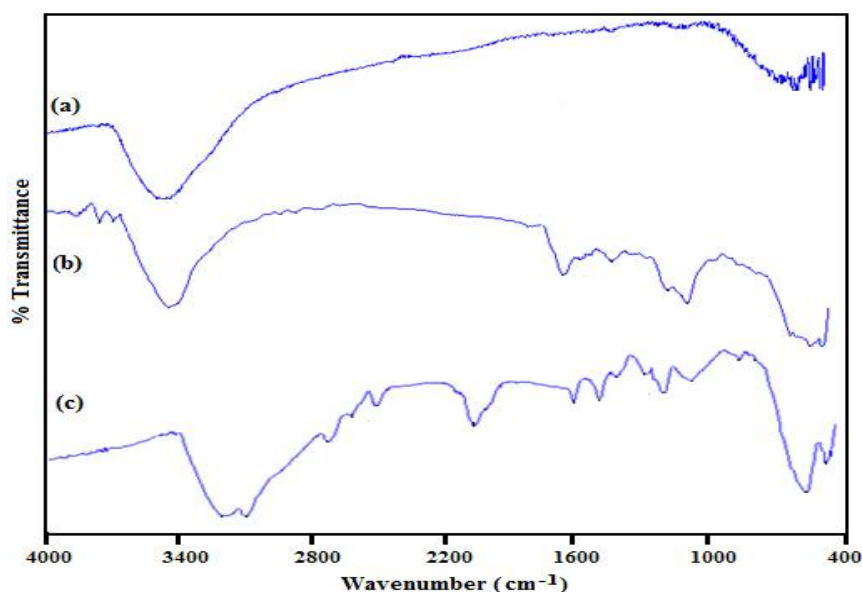


Figure 3: ATR-FTIR spectrums of (a) pure CFNPs; (b) xanthan gum coated (CoFe₂O₄.NPs@XG); and (c) doxorubicin loaded cobalt ferrite NPs (CoFe₂O₄.NPs@XG-Dox)

Thermal characteristics

Thermal analysis of the uncoated and coated CFNPs was performed from 25 to 800 °C to obtain quantitative evidence of the nanoferrite coating. The TGA curves of the pure and XG-coated ferrite NPs displayed different thermal behaviours (Figure 4). The percentage weight loss of the uncoated ferrite nanocrystals was just 3 % over the range of 20 – 200 °C. However, the XG-coated CFNPs exhibited a ca. 8% mass loss below 150°C, which increased to ca. 16 % from 150 to 380 °C.

Contact angle

The wettability and surface interactions of the coated and uncoated CFNPs with water were determined by contact angle measurements. CFNPs should be hydrophilic for biomedical applications. Figure 4 shows the sessile water droplet (2 μ L) contact angles over thick solid sample surfaces. The contact angles of the native and XG-coated ferrite NPs were 92.40° and 39.90°, respectively (Figure 5 (a, b)).

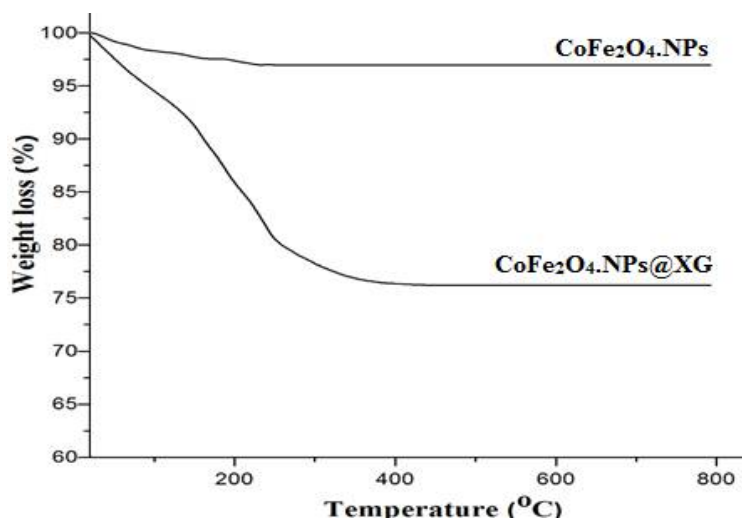


Figure 4: Thermogravimetric curves for native ($\text{CoFe}_2\text{O}_4\text{.NPs}$) and xanthan gum coated cobalt ferrite nanoparticles ($\text{CoFe}_2\text{O}_4\text{.NPs@XG}$)

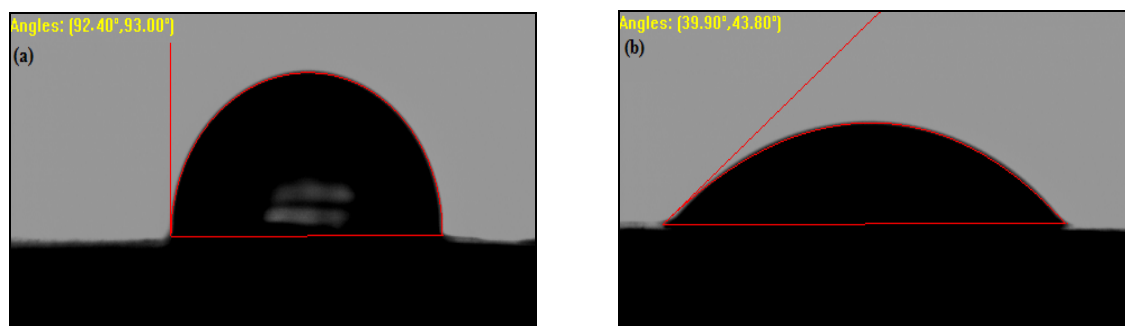


Figure 5: Contact angle images of (a) uncoated $\text{CoFe}_2\text{O}_4\text{.NP}$; (b) XG-coated cobalt ferrite NPs ($\text{CoFe}_2\text{O}_4\text{.NPs@XG}$) for comparison of their wettability with water droplet

XRD

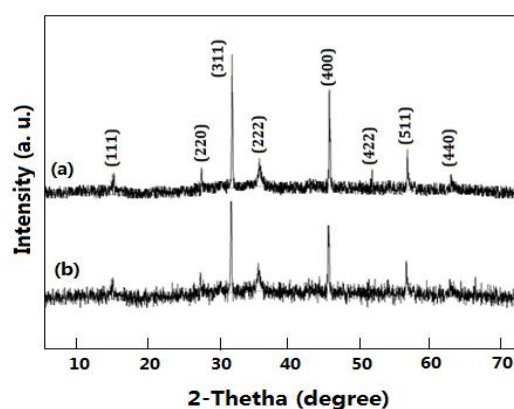


Figure 6: XRD patterns of (a) uncoated $\text{CoFe}_2\text{O}_4\text{.NPs}$ and (b) xanthan gum-coated $\text{CoFe}_2\text{O}_4\text{.NPs@XG}$ (b)

Figure 6 shows the XRD patterns of the uncoated ($\text{CoFe}_2\text{O}_4\text{.NPs}$) and XG-coated ($\text{CoFe}_2\text{O}_4\text{.NPs@XG}$) CFNPs. For the uncoated case, the (111), (220), (311), (222), (400), (422), (511) and (440) diffraction planes corresponded to angles of 18.29° , 30.08° , 35.44° , 37.06° , 43.06° , 53.45° , 56.98° and 62.59° , respectively. The indexed values of the uncoated CFNPs were

in agreement with the Joint Committee on Powder Diffraction Standards (JCPDS) data card no. 22-1086 for the inverse spinel structure having a cubic geometry. The same characteristic XRD peaks were also observed for the XG-coated CFNPs (Figure 6 (b)), also indicating the single-phase spinel structure for the coated sample. The average crystal size (D) of the uncoated $\text{CoFe}_2\text{O}_4\text{.NPs}$ was 18 nm.

Morphology

SEM, AFM and DLS were used to investigate the microstructure of the uncoated and XG-coated CFNPs. SEM images (Figure 7 (a, b)) reveal the elongated, oval-shaped morphology of the native ferrite NPs. The average size of the native and coated CFNPs ranged from 20 to 60 nm. Topographical images of the uncoated and coated $\text{CoFe}_2\text{O}_4\text{.NPs}$ are shown in Figure 8 (a, b). Furthermore, the 3-D AFM image (Figure 8c) confirmed the oval-shaped texture of the uncoated CFNPs, as previously noted [18]. DLS measurements (Figure 9) established a PDI of less than 0.16 and a nanosized range for all of the prepared samples [9].

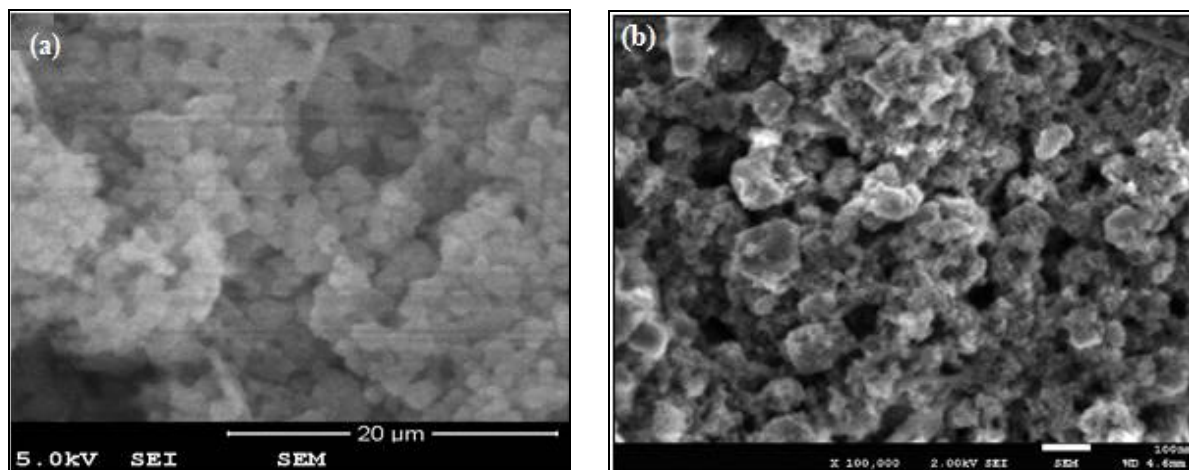


Figure 7: SEM images of uncoated (a); and XG-coated Cobalt ferrite NPs (b)

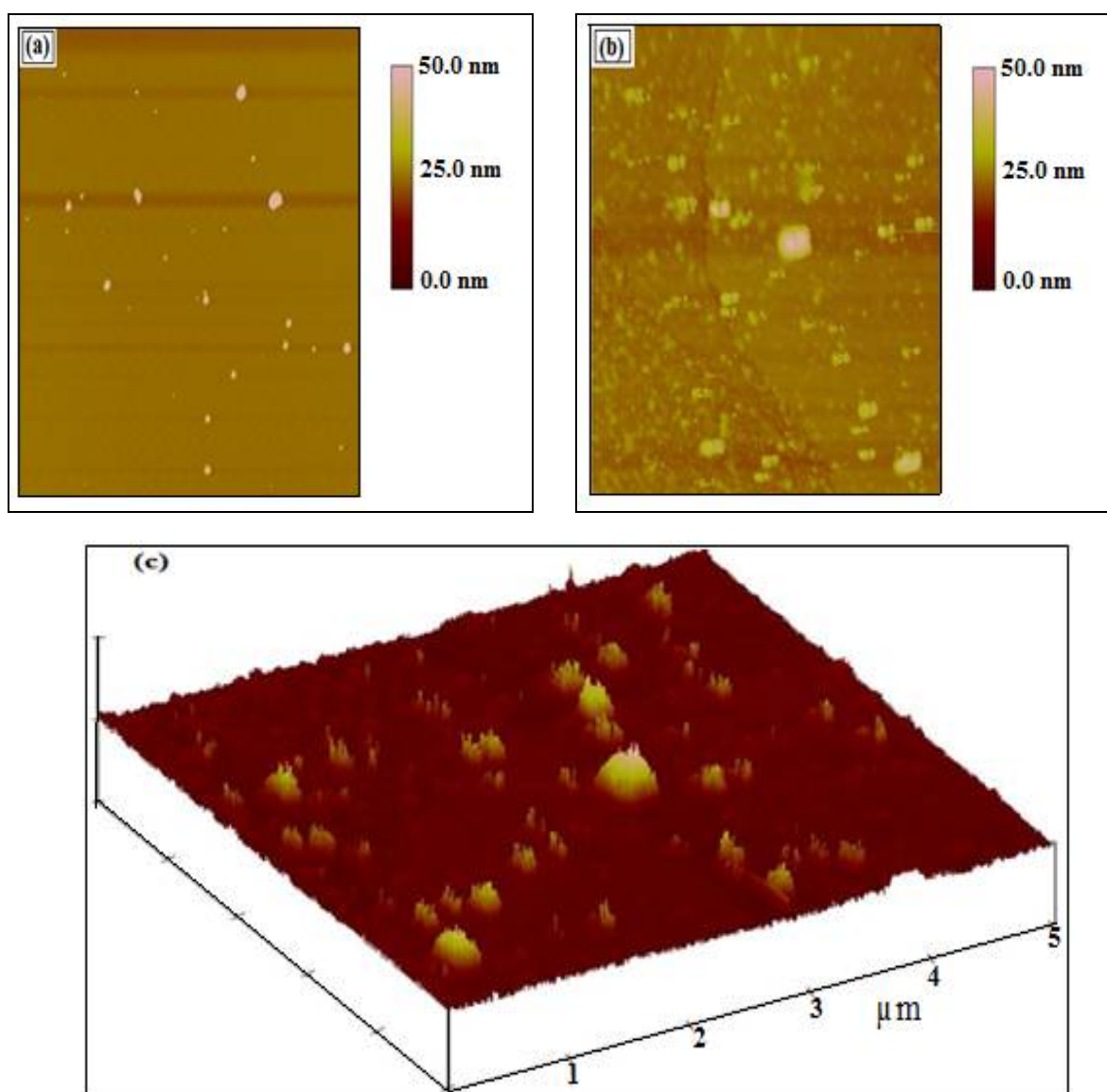


Figure 8: Topographical AFM images of (a) uncoated; (b) XG-coated Cobalt ferrite NPs; (c) 3D AFM image of native CoFe₂O₄.NPs

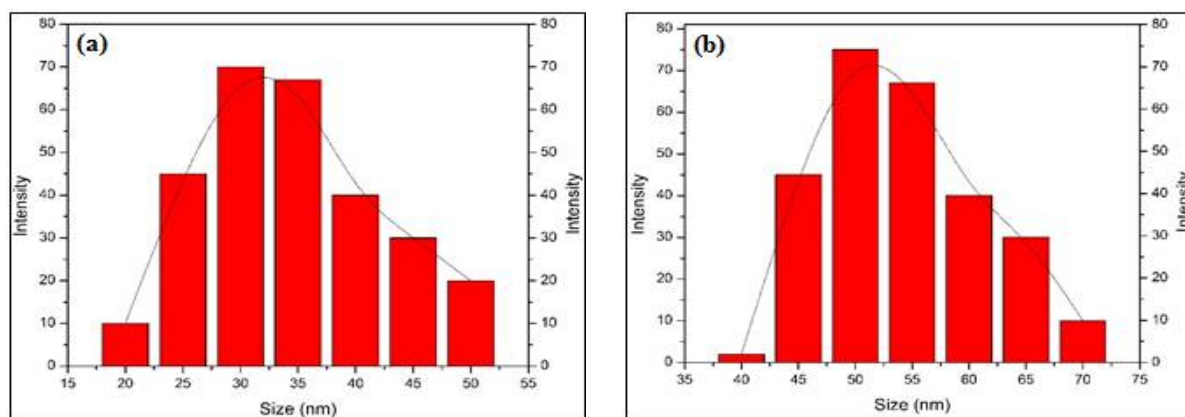


Figure 9: Size histogram images of (a) uncoated; (b) XG-coated Cobalt ferrite NPs obtained from DLS measurements

Magnetic properties

The magnetic properties of the uncoated and XG-coated CFNPs were measured by VSM at room temperature. Figure 10 shows the magnetisation as a function of the applied field ($M-H$ curves) of the coated and uncoated CFNPs for magnetisation varying from -15 to 15 kOe. VSM study produced M_s values of 62.55 and 50.27 emu/g for the uncoated and coated CFNPs, respectively. A suspension of pure CFNPs showed a strong attraction toward a magnetic field (Figure 11).

Drug release profile

The anti-tumour drug release profile of the drug-loaded MNV was determined in the absence and presence of an external AMF. The Doxo encapsulation efficiency of the

$\text{CoFe}_2\text{O}_4\text{.NPs@XG}$ MNV was ca. 83 %, which is greater than previously reported [19]. Wong *et al.* reported an average encapsulation efficiency of ca. 70 % for Doxo on solid lipid nanoparticles (SLNs) [20]. The drug release behaviour of the MNV was studied for 120 h in phosphate-buffered saline (0.1 M) at two different pHs (7.4 and 5.0) at 37°C (Figure 12 (a, b)). The pH of 7.4 corresponds to the normal environment of body tissue and blood, while pH 5.0 is more appropriate for tumour-affected cells [21]. The drug-loaded MNV ($\text{CoFe}_2\text{O}_4\text{.NPs@XG}$ -Doxo) did not show a significant release of Doxo at neutral pH 7.4 in the absence (13.5 %) as well as presence (32 %) of AMF after 120 h. In contrast, at pH 5.0, the discharge of drug was slow (ca. 15 %) in the first 6 h, which increased to 39 % after 120 h. However, an increased, controlled and regular release of drug up to 69% was observed in the presence of the external AMF after 120 h.

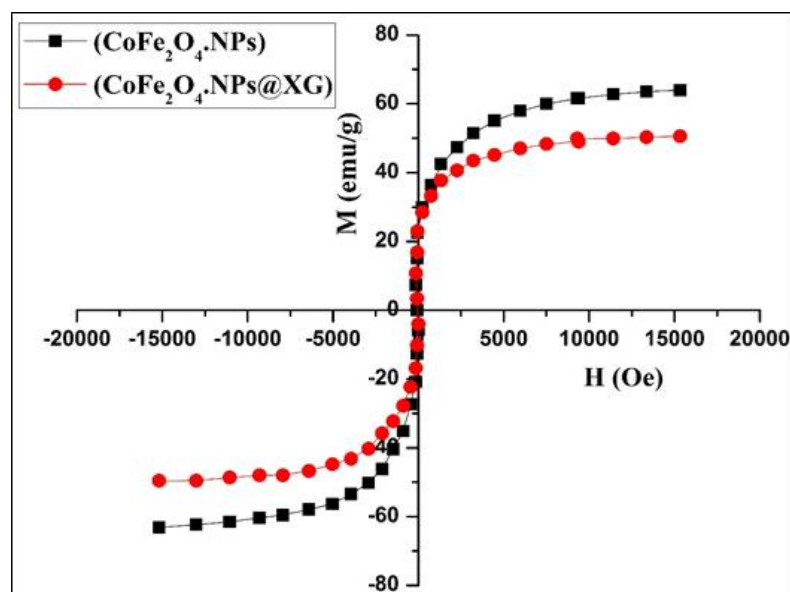


Figure 10: Vibrating sample magnetometer graphs of uncoated ($\text{CoFe}_2\text{O}_4\text{.NPs}$) and XG-coated Cobalt ferrite NPs ($\text{CoFe}_2\text{O}_4\text{.NPs@XG}$)

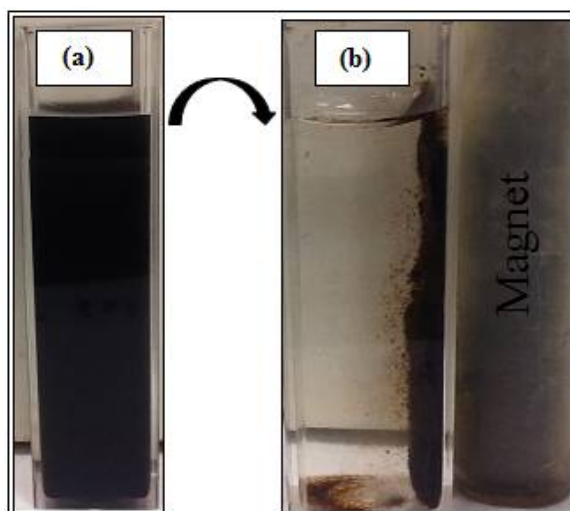


Figure 11: CoFe₂O₄.NPs suspension (a); which is exhibiting magnetic response towards a magnet (b)

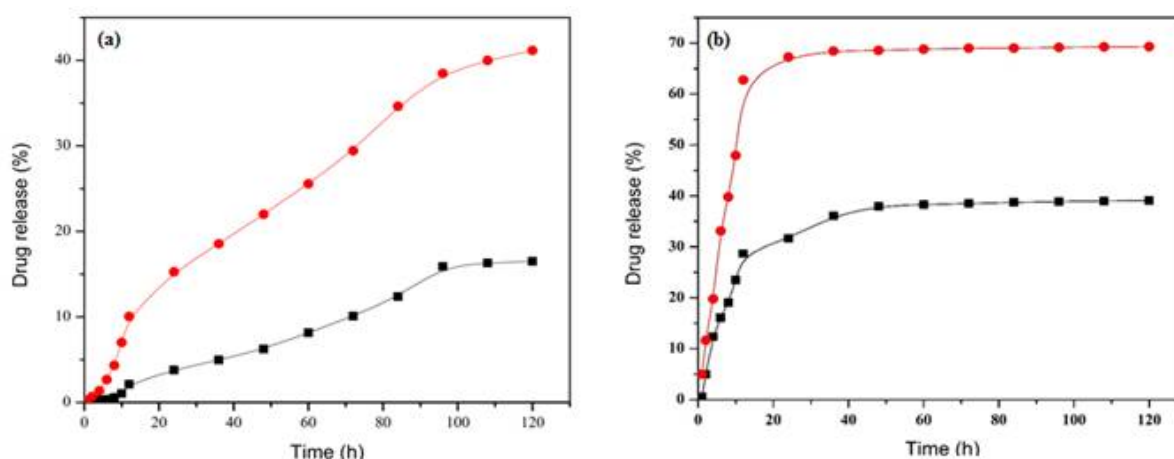


Figure 12: Drug release profile in the absence (■) and presence (●) of externally applied magnetic field (AMF) at (a) pH ~ 7.4; (b) pH ~ 5.0

***In vitro* toxicity of CoFe₂O₄.NPs@XG**

The MTT assay against the CHO and Huh7 cell lines was used to establish the *in vitro* toxicity of the XG-coated ferrite NPs. Figure 13 exhibits the cell viability profiles of the CHO and Huh7 cells incubated at various concentrations (0–2.0 mg/mL) of MNV. After 48 h of dose exposure, cell viability exceeding 80 %, even at a high concentration (1.6 mg/mL), confirmed the biocompatibility of the CoFe₂O₄.NPs@XG. This is likely because XG is a food-grade polysaccharide whose degradation products are not toxic to the exposed cells.

Pharmacological activity of CoFe₂O₄.NPs@XG-Doxo

A 0–0.18 mg/mL dose of the drug-loaded MNA (CoFe₂O₄.NPs@XG-Doxo) was applied to Huh7 cells over 48 h of incubation to investigate its pharmacological activity. Figure 14 reveals the

significant decrease in the percentage cell viability with increasing concentration of the magnetic nanoassembly. More than 50 % of the cells were dead even at the low concentration of 0.16 mg/mL. This marked decrease in cell viability was attributed to the anti-proliferative effect of the Doxo discharged from the MNA.

DISCUSSION

The UV-vis absorption band in the range of 330–500 nm was attributed to the homogenised electronic motion of the CFNPs. Generally, metal nanoparticles display a characteristic plasmon resonance band in their UV-vis absorbance spectra due to the collective resonance of their conduction electrons [19]. Peaks in the range of 400–600 cm⁻¹ for metal ferrite NPs indicate the presence of a metal–oxygen bond. The splitting of the low-frequency band for the octahedral site (B) reveals the presence of different metal ions including Fe³⁺, Fe²⁺ and Co²⁺.

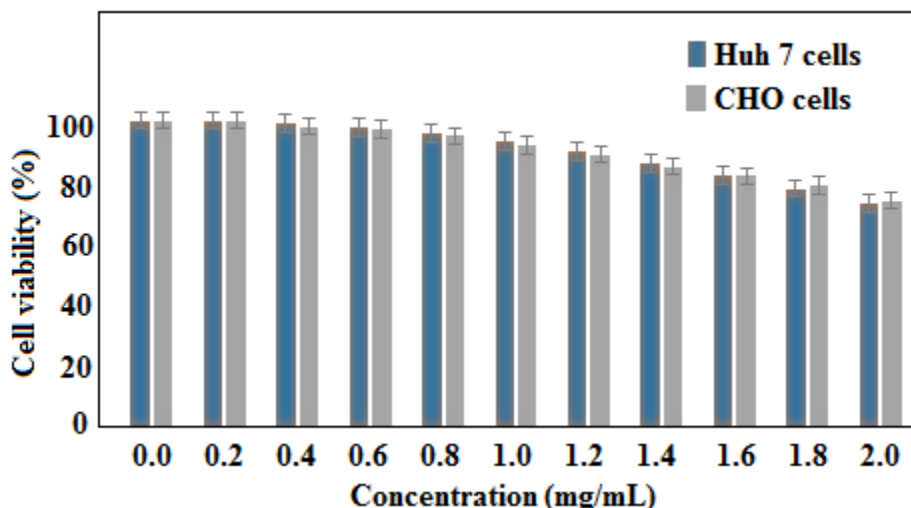


Figure 13: Pharmacological activity of xanthan gum coated CoFe_2O_4 .NPs@XG against CHO and Huh 7 cells

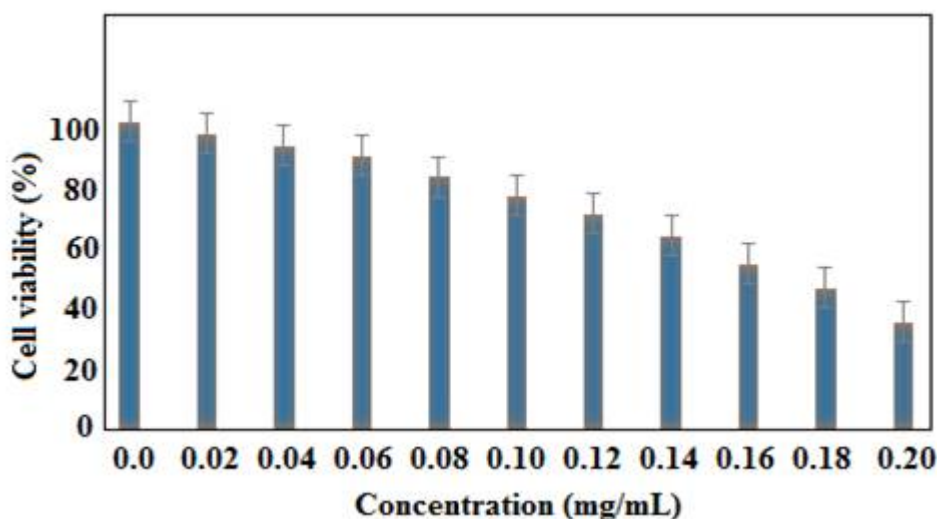


Figure 14: Pharmacological activity of doxorubicin loaded CFNPs (CoFe_2O_4 .NPs@XG-Doxo) against Huh 7

However, the slight shifting of the M–O peaks of the coated CFNPs was attributed to the polymeric XG layer. The broad absorption band at $3350\text{--}3500\text{ cm}^{-1}$ was assigned to the stretching vibration of the –OH group. The splitting of the peaks at $2950\text{--}3250$ and 1547 cm^{-1} corresponds to the N–H stretching and N–H bending vibrations, respectively, of the secondary amide group. Briefly, the FT-IR spectrum of the loaded drug (Figure 3c) revealed drug adsorption in two ways: first, by the partial interaction between the XG carboxylate (COO^-) and amine ($-\text{NH}_2$) groups of the drug *via* amide formation and, second, by the –OH vibrational bands [21].

The percentage weight loss determined by TGA of the pure CFNPs was attributed to the evaporation of absorbed water and ethanol from the nanoferrite powder surface. Such a small change in mass was consistent with the pure spinel phase of the CFNPs. The mass loss of the XG-coated CFNPs was mostly observed in two

regions. The first mass loss was due to the loss of loosely bound water molecules and the coated layer of polymer. However, the second step of a sharp mass loss corresponded to the combustion of the polymer coating from the NP surface [22].

Coating with XG is an effective way to reduce the hydrophobicity of ferrites and increase their water dispersibility. Indeed, the presence of abundant hydroxyl (–OH) and carboxyl (–COOH) groups in XG increases the porosity and surface energy of XG-coated magnetic NPs, and increases their hydrophilicity [23].

The XRD spectra of the native CFNPs (CoFe_2O_4 .NPs) confirmed their crystalline nature with the inverse spinel structure and the space group $Fd3m, O_h$. The absence of *hkl* planes of iron or cobalt oxides (Fe_2O_3 , Fe_3O_4 , CoO) indicated the purity of the synthesised CFNPs [24]. However, the negligible crystallinity observed for the CoFe_2O_4 .NPs@XG was caused

by the amorphous layer of XG that coated the CFNPs.

SEM images of the uncoated CFNPs revealed some agglomeration that was attributed to van der Waals forces and dipole-dipole magnetic attractions [25]. However, the XG-coated CFNPs were less agglomerated and had lower polydispersity.

The absence of a hysteresis loop, and negligible remanence (M_r) and coercivity (H_c) reflected the superparamagnetic behaviour of the CFNPs. The lower M_s value of the coated CFNPs ($\text{CoFe}_2\text{O}_4\text{.NPs@XG}$) may be correlated with various factors such as the low mass and small size of the magnetic core and the presence of the magnetically inactive XG layer, which reduced the exchange coupling energy of the magnetic field [26]. Additionally, the high magnetisation value of the native CFNPs reflected their uniform distribution and small degree of agglomeration.

CONCLUSION

Superparamagnetic nanocrystals of cobalt ferrite has been readily synthesised by co-precipitation with their surface was modified by XG, a food-grade hydrophilic polymer. Various analyses confirmed the presence of M–O bond and bonding of XG functional groups to the surface of the CFNPs. The superparamagnetic behaviour (negligible coercivity, remanence and hysteresis at 300 K) of the bare CFNPs is preserved in the XG-coated CFNPs ($\text{CoFe}_2\text{O}_4\text{.NPs@XG}$), which suggests its potential as an MNV for anti-cancer drugs. Significantly enhanced release of Doxo from $\text{CoFe}_2\text{O}_4\text{.NPs@XG}$ -Doxo in the presence of an AMF has been achieved. The XG-coated CFNPs are biocompatible while the drug-loaded MNV assembly, $\text{CoFe}_2\text{O}_4\text{.NPs@XG}$ -Doxo, efficiently inhibits cell viability, which suggests intracellular uptake of Doxo by Huh7 cancer cells. Thus, surface modification of CFNPs with XG is a novel technique to obtain a cytocompatible MNV to deliver Doxo to targeted sites.

DECLARATIONS

Acknowledgement

This research was conducted with funding provided by the Higher Education Commission (HEC) of Pakistan. The authors acknowledge the support of Dr Bushra Ijaz and other staff members of the Centre of Excellence in Molecular Biology (CEMB), University of the Punjab, Lahore, Pakistan.

Conflict of Interest

No conflict of interest associated with this work.

Contribution of Authors

The authors declare that this work was done by the authors named in this article and all liabilities pertaining to claims relating to the content of this article will be borne by them.

Open Access

This is an Open Access article that uses a funding model which does not charge readers or their institutions for access and distributed under the terms of the Creative Commons Attribution License (<http://creativecommons.org/licenses/by/4.0>) and the Budapest Open Access Initiative (<http://www.budapestopenaccessinitiative.org/read>), which permit unrestricted use, distribution, and reproduction in any medium, provided the original work is properly credited.

REFERENCES

- Guo W, Wu L, Chen Z, Boschloo G, Hagfeldt A, Ma T. Highly efficient dye-sensitised solar cells based on nitrogen-doped titania with excellent stability. *J. Photochem. Photobiol. A: Chem.* 2011; 219: 180–187.
- Huang J, Zhong X, Wang L, Yang L, Mao H. Improving the magnetic resonance imaging contrast and detection methods with engineered magnetic nanoparticles. *Theranostics* 2012; 2: 86.
- Yan CH, Xu ZG, Cheng F X, Wang ZM, Sun LD, Liao CS, Jia JT. Nanophased CoFe_2O_4 prepared by combustion method. *Solid State Commun.* 1999; 111: 287–291.
- Moumen N, Veillet P, Pileni M. Controlled preparation of nanosize cobalt ferrite magnetic particles. *J. Magn. Mater.* 1995; 149: 67–71.
- Ngo AT, Bonville P, Pileni MP. Synthesis and superparamagnetic properties of Nanoparticles. *Eur. Phys. J. B - Condensed Matter and Complex Systems* 1999; 9: 583–592.
- Dey S, Ghose J. Synthesis, characterisation and magnetic studies on nanocrystalline $\text{Co}_0.2\text{Zn}_0.8\text{Fe}_2\text{O}_4$. *Mater. Res. Bull.* 2003; 38: 1653–1660.
- Sathaye SD, Patil KR, Kulkarni SD, Bakre PP, Pradhan SD, Sarwade BD, Shintre SN. Modification of spin coating method and its application to grow thin films of cobalt ferrite. *J. Mater. Sci.* 2003; 38: 29–33.
- Sorescu M, Diamandescu L, Peelamedu, R, Roy R, Yadoji P. Structural and magnetic properties of Nisn ferrites prepared by microwave sintering. *J. Magn. Mater.* 2004; 279: 195–201.
- Mathieu A, Lotfi Ben T, Frederic H, Leila S, Francoise V, Nader Y, Jean-Marc G, Souad A, Fernand F. Size-dependent magnetic properties of CoFe_2O_4

- nanoparticles prepared in polyol. *J. Phys. Condens. Matter* 2011; 23: 506001.
10. Davis SS. Biomedical applications of nanotechnology-implications for drug targeting and gene therapy. *Trends Biotechnol.* 1997; 15: 217–24.
 11. Nappini S, Magnano E, Bondino F, Pis I, Barla A, Fantechi E, Pineider F, Sangregorio C, Vaccari, L, Venturelli L. Surface charge and coating of CoFe_2O_4 nanoparticles: Evidence of preserved magnetic and electronic properties. *J. Phys. Chem. C* 2015; 119: 25529–25541.
 12. Salunkhe AB, Khot VM, Thorat ND, Phadatare MR, Sathish CI, Dhawale DS, Pawar SH. Polyvinyl alcohol functionalised cobalt ferrite nanoparticles for biomedical applications. *Appl. Surf. Sci.* 2013; 264: 598–604.
 13. Mushtaq MW, Kanwal F, Bashir S, Imran M, Synthesis, Characterisation and biological studies of cobalt ferrite nanoparticles. *Bul. Chem. Commun.* 2016; 48: 565–570.
 14. Akbarzadeh A, Zarghami N, Mikaeili H, Asgari D, Goganian AM, Khiabani HK, Samiei M, Davaran S, Synthesis, characterisation and in vitro evaluation of novel polymer-coated magnetic nanoparticles for controlled delivery of doxorubicin. *Nanotechnol. Sci. Appl.* 2012; 5: 13–25.
 15. Wang G, Ma Y, Mu J, Zhang Z, Zhang X, Zhang L, Che H, Bai Y, Hou J, Xie H. Monodisperse polyvinylpyrrolidone-coated CoFe_2O_4 nanoparticles: Synthesis, characterisation and cytotoxicity study. *Appl. Surf. Sci.* 2016; 365: 114–119.
 16. Mahmoudi M, Simchi A, Imani M, Milani AS, Stroeve P. Optimal design and characterisation of superparamagnetic iron oxide nanoparticles coated with polyvinyl alcohol for targeted delivery and imaging. *J. Phys. Chem. B* 2008; 112: 14470–14481.
 17. Aronniemi M, Lahtinen J, Hautajarvi P. Characterisation of iron oxide thin films. *Surf. Interface Anal.* 2004; 36: 1004–1006.
 18. Che E, Wan L, Zhang Y, Zhao Q, Han X, Li J, Liu J, Wang S. Development of phosphonate-terminated magnetic mesoporous silica nanoparticles for pH-controlled release of doxorubicin and improved tumour accumulation. *Asian J. Pharm. Sci.* 2014; 9: 317–323.
 19. Wong HL, Rauth AM, Bendayan R, Manias JL, Ramaswamy M, Liu Z, Erhan SZ, Wu XY. A new polymer-lipid hybrid nanoparticle system increases cytotoxicity of doxorubicin against multidrug-resistant human breast cancer cells. *Pharm. Res.* 2006; 23: 1574–1585.
 20. Arsalani N, Fattahi H, Nazarpour M, Synthesis and characterisation of PVP-functionalised superparamagnetic Fe_3O_4 nanoparticles as an MRI contrast agent. *Express Polym. Lett.* 2010; 4: 329–338.
 21. Zhang Y, Das GK, Xu R, Yang Tan TT. Tb-doped iron oxide: bifunctional fluorescent and magnetic nanocrystals. *J. Mater. Chem.* 2009; 19: 3696–3703.
 22. Liu G, Hong RY, Guo L, Li YG, Li HZ. Preparation, characterisation and MRI application of carboxymethyl dextran coated magnetic nanoparticles. *Appl. Surf. Sci.* 2011; 257: 6711–6717.
 23. Huang Z, Zhu Y, Zhang J, Yin G. Stable biomimetic super hydrophobicity and magnetisation film with Cu-ferrite nanorods. *J. Phys. Chem. C* 2007; 111: 6821–6825.
 24. Khandekar MS, Kambale RC, Patil JY, Kolekar YD, Suryavanshi SS. Effect of calcination temperature on the structural and electrical properties of cobalt ferrite synthesised by combustion method. *J. Alloys Compd.* 2011; 509: 1861–1865.
 25. Zhang X, Guo Q, Cui D. Recent advances in nanotechnology applied to biosensors. *Sensors* 2009; 9: 1033–1053.
 26. Raghavender A. Synthesis and characterisation of cobalt ferrite nanoparticles. *Sci. Technol. Arts Res. J.* 2014; 2: 1–4.